Supporting Information

Photothermal synergy mechanism in near-infrared photopolymerization for 3D printing acceleration and mechanical enhancement

Wei Wu [a], *Hang Xu* [a], *Jia-Tao Miao* [a, b], *Xiucheng Zou* [a, b, *], *Ren Liu* [a, b, *]

[a] Key Laboratory of Synthetic and Biological Colloids, Ministry of Education, School of Chemical and Material Engineering, Jiangnan University, 214122, Wuxi, Jiangsu, China.

[b] International Research Center for Photoresponsive Molecules and Materials, Jiangnan University, 214122, Wuxi, Jiangsu, China.

* Corresponding authors.

E-mail address:liuren@jiangnan.edu.cn(R, Liu), zouxiucheng@jiangnan.edu.cn(X, Zou).

1. Experimental Section

1.1 Materials

1.2 Characterizations

1.3 Root mean square roughness

2. Figures

1. Experimental Section

1.1 Materials

Difunctional bisphenol-A epoxy acrylate oligomer (RY1101), tri(propyleneglycol)diacrylate (TPGDA), trimethylolpropane triacrylate (TMPTA) were purchased from Jiangsu Kailinruiyang Chemical Co., Ltd. (China). Ethoxylated bisphenol-A diacrylate (EM2261) was purchased from Eternal Synthetic Resins Co., Ltd. (China). Phenyl bis(2,4,6-trimethylbenzoyl)-phosphine oxide (BAPO) was purchased from Gurun Technology Co., Ltd. (China), and UCPs (NaYF4: Yb, Tm. 81.5 mol% Y, 18 mol% Yb, 0.5 mol% Tm) were purchased from Shanghai Ziqi Chemical Technology Co., Ltd. The thermal initiators azo diisobutyronitrile (ABVN), azo diisobutyronitrile (AIBN), p-benzoyl peroxide (BPO), and tert-butyl peroxybenzoate (TBPB) were supplied by Shanghai Adamas Reagent Co., Ltd. All reagents were used without further purification unless otherwise stated.

1.2 Characterizations

scanning electron microscope images were monitored with a Hitachi S-4800 SEM. UV-vis spectra were measured using a Beijing Purkinje TU-1901 UV−vis spectrophotometer. Real-time monitoring of temperature was performed using a Fluke Ti400 thermal imager. The dissociation temperatures of thermal initiators were measured using Mettler Q200 DSC. Tensile properties were measured by using a universal Instron 5967X Universal Testing Systems. Five specimens of each sample

were tested, and the averaged results were presented. The surfaces of the samples were observed using an upper light source with an ultra-depth of field VHX-1000C microscope, and digital photographs were taken. Raman spectra and mapping images of the sample surface were obtained using a 532 nm laser and a 20x objective on a DXR3xi (ThermoFisher, USA) confocal Raman microscope system. An area of 30 μm × 200 μm was scanned in 2 μm steps to obtain 16 × 100-pixel images. The equation for calculating the double bond conversion ratio is the same as that listed for the double bond conversion ratio. The viscosity of the uncured resin was measured with a HAAKE MARS60 rheometer equipped with Rheonaut annex (ThermoFisher), exhibiting a cone-and-plate geometry (50 μm gap) with a 20 mm diameter and 2° angle. The temperature was controlled with the help of an integrated Peltier unit.

1.3 Root mean square roughness

Morphology investigations were performed on the surfaces of the cured samples using atomic force microscopy (AFM, MuLtimode 8). The image processing software (Nanoscope Analysis 3.0) was used to perform topography fitting and compute root-mean-square roughness (*Rq*). *Rq* is defined as the standard deviation of Z values in a given region, which is calculated using the following formula:

$$R_q = \sqrt{\frac{\sum (z_t - z_a)^2}{n}}$$

2. Figures

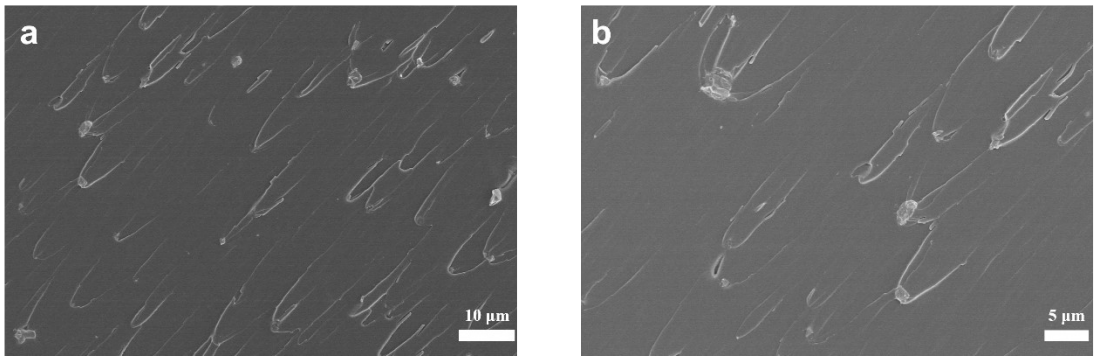

Fig. S1. SEM images of the cross-section of a tensile strip. Uniform distribution of UCPs was observed at all magnifications.

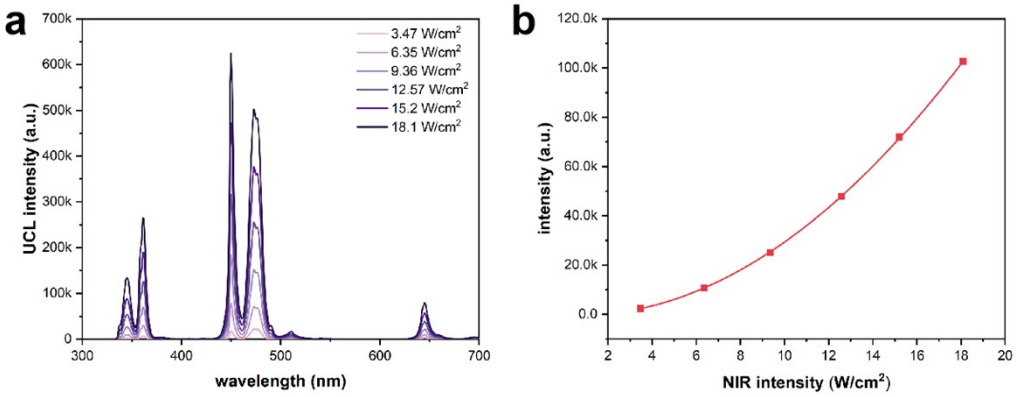

Fig. S2. (a) UCPs fluorescence emission spectra under different near-infrared light intensities. (b) Dependence of UCPs fluorescence intensity on excitation light intensity at 330-370 nm.

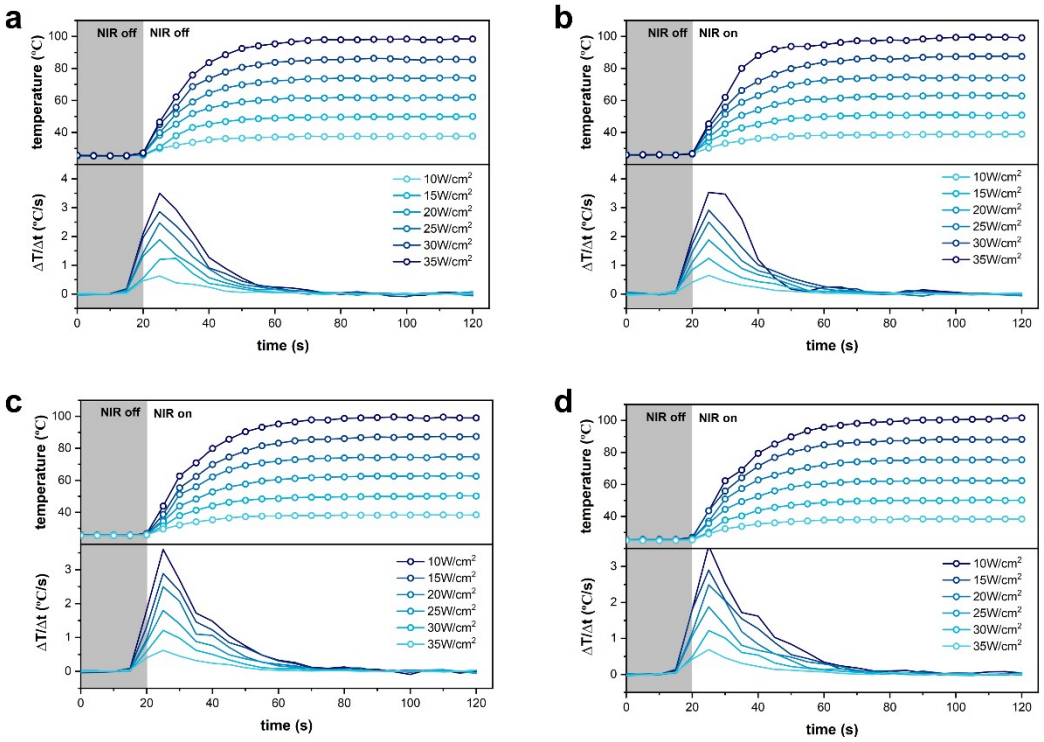

Fig. S3. Temperature-time curves and temperature rate-time curves of systems with (a) 0.25 wt.%, (b) 0.5 wt.%, (c) 1 wt.% and (d) 2 wt.% PIs. When only PIs is added, the temperature and heating rate of the system do not change significantly with the increase of PIs concentration.

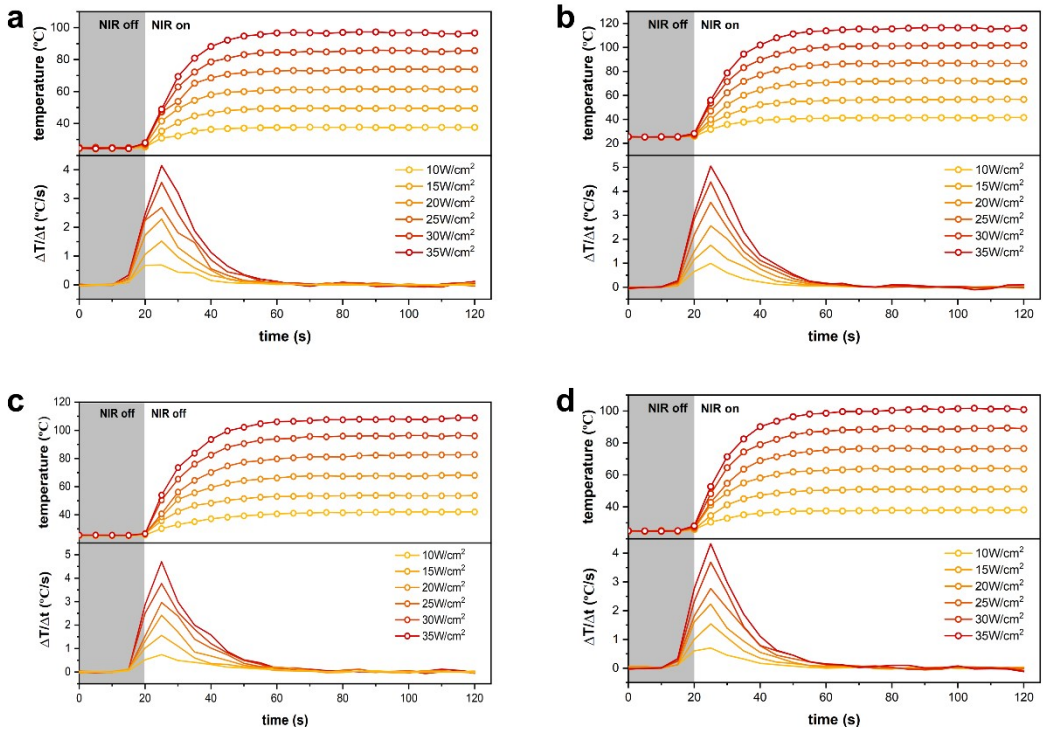

Fig. S4. Temperature-time curves and temperature rate-time curves of systems with (a) 0.25 wt.%, (b) 0.5 wt.%, (c) 1 wt.% and (d) 2 wt.% UCPs. The increase of UCPs concentration significantly increases the temperature and heating rate of the system, indicating that the UCPs concentration is an important factor affecting the thermal effect of the system.

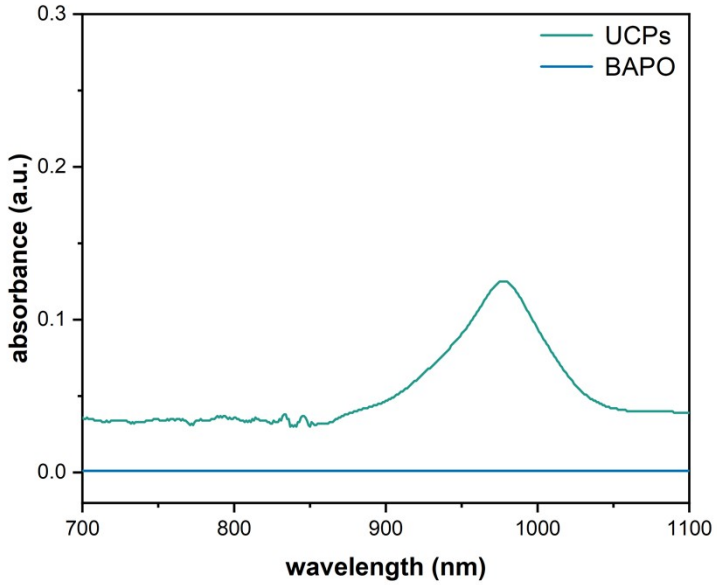

Fig. S5. The absorption spectra of UCPs and BAPO at 700 to 1100nm. As can be seen, there is a significant absorption at 980 nm for UCPs, but not for BAPO

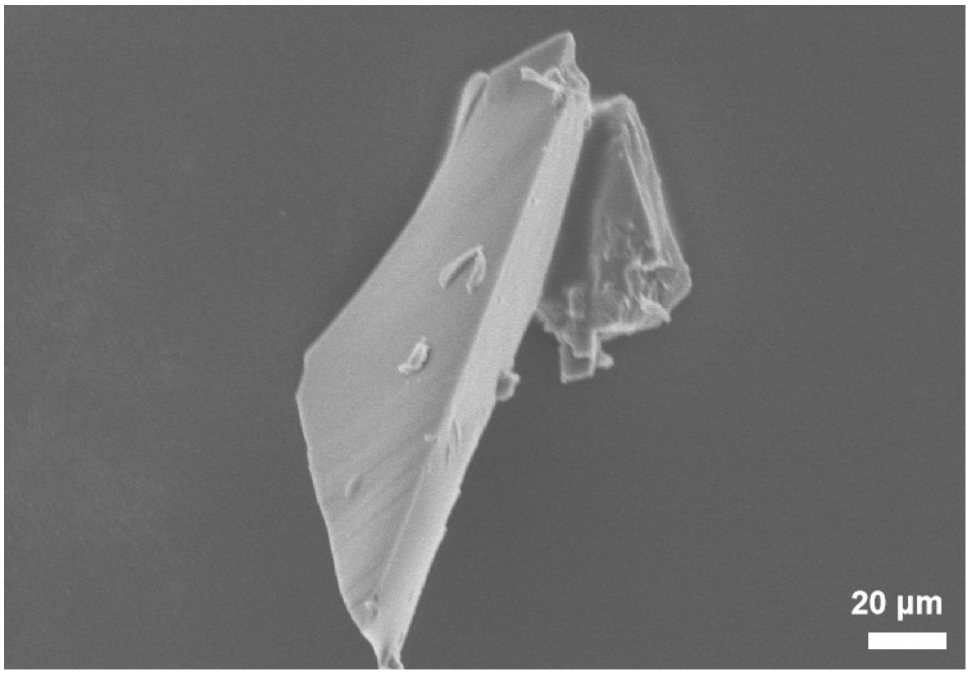

Fig. S6. The SEM images of UCPs with polymer appearing on the surface.

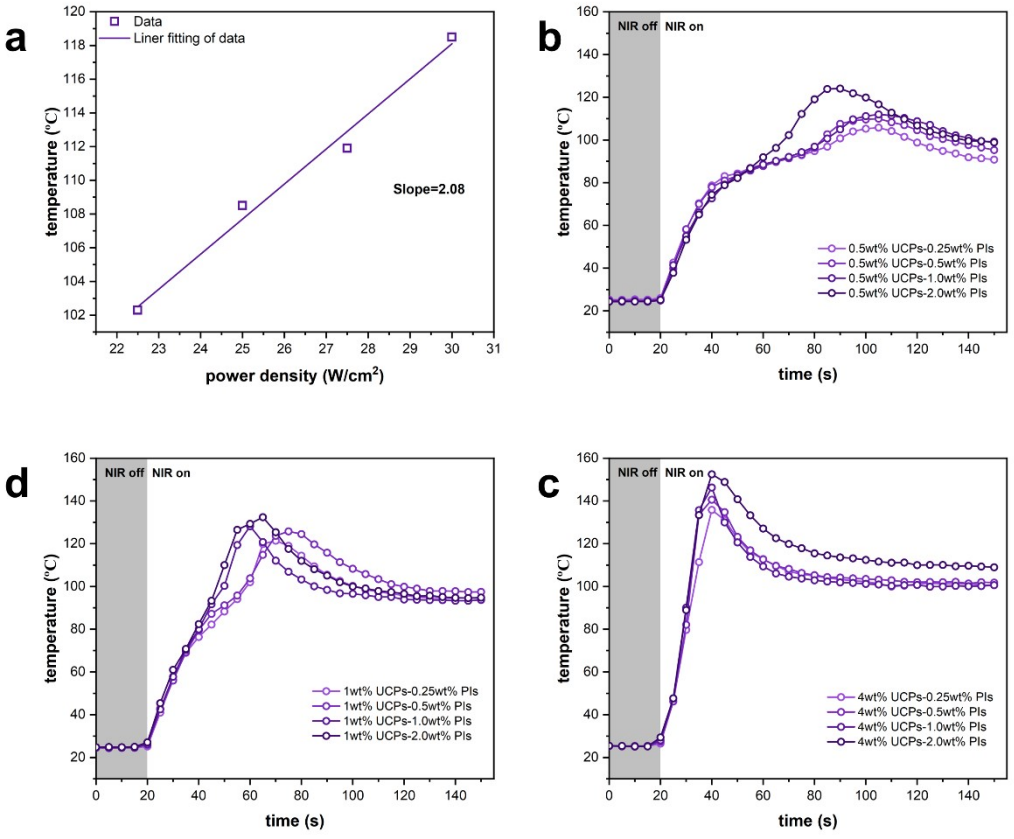

Fig. S7. (a) T_p as a function of power density of UCAP system containing 2 wt.% UCPs and 0.5 wt.% PIs. Temperature-time curves of UCAP system containing different PIs

concentrations at (b) 0.5 wt.% UCPs, (c) 1 wt.% UCPs, (d) 4 wt.% UCPs. The power density of NIR laser is 30 W/cm^2. When polymerization occurs, the T_p of the system maintains a linear relationship with the laser power density, so the T_p of the system can be adjusted by adjusting the power density. Increasing the concentration of UCPs and PIs increases the temperature of the system.

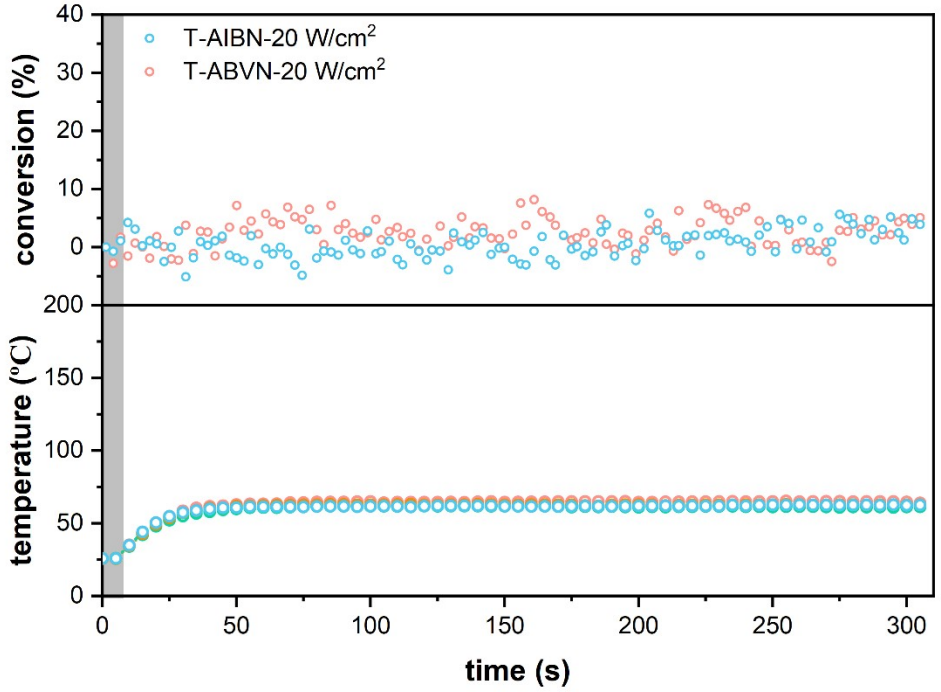

Fig. S8. Conversion-time curves and temperature-time curves of thermal curing system under the power density of 20 W/cm^2 (0.25 wt.% TIs). When the power density is low, there is no polymerization due to the absence of polymerization heat.

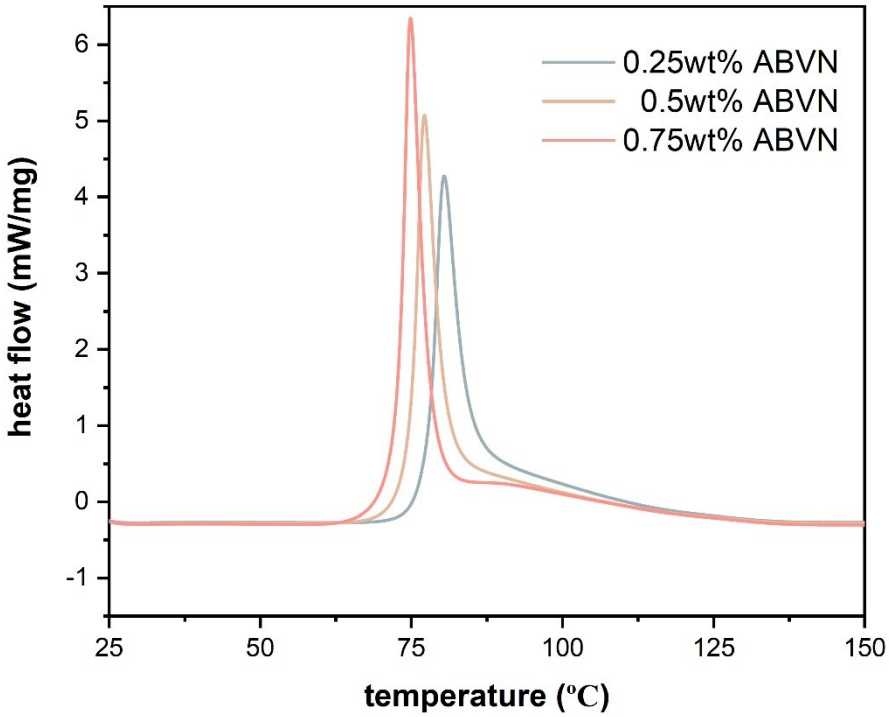

94

95 **Fig. S9.** DSC curves of different concentrations of ABVN with a temperature rise of

96 10 K/min. With the increase of the concentration of thermal initiator, T_d decreased and

97 the polymerization rate of thermal polymerization increased.

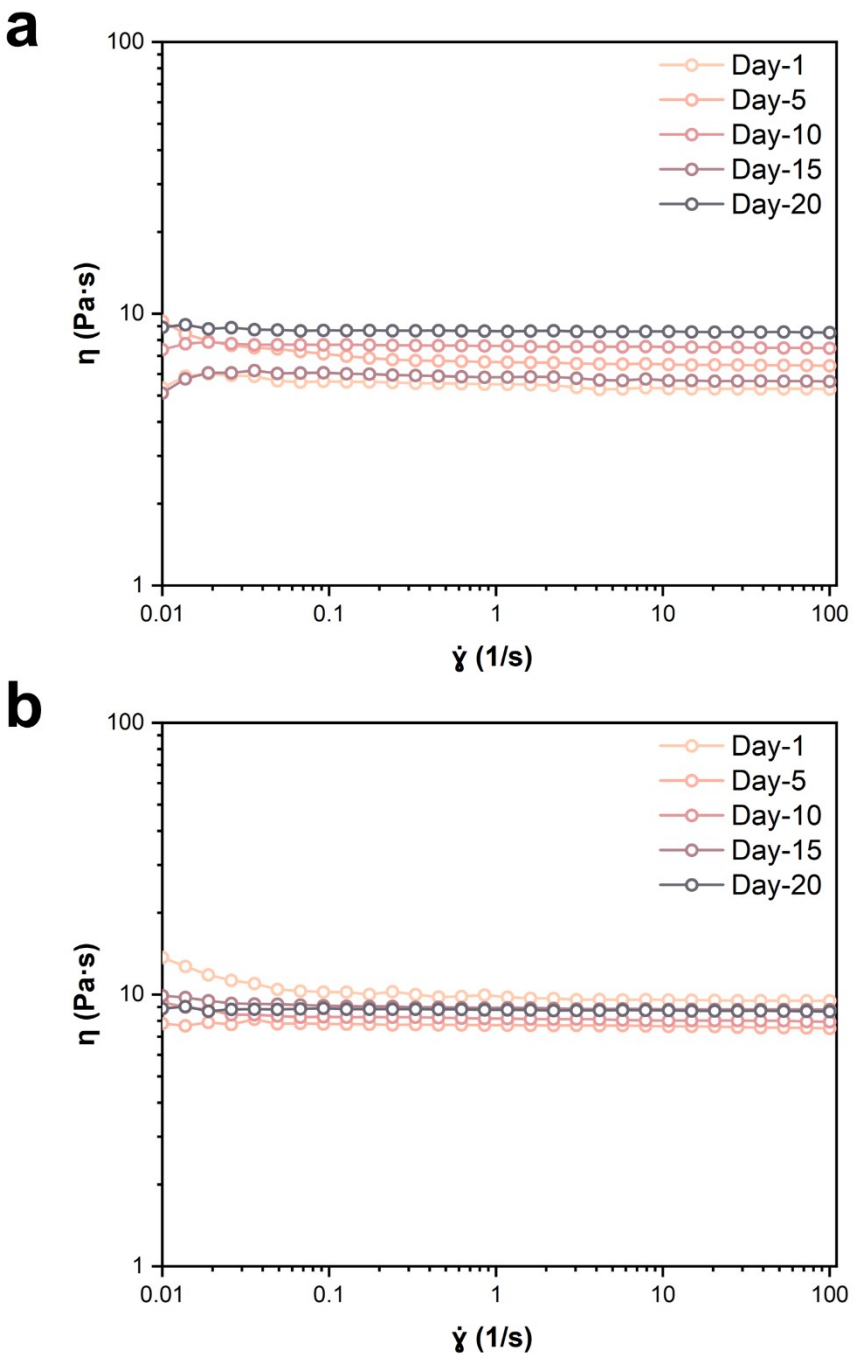

Fig. S10. (a) Viscosity curves of PT-ABVN formulation for different days at 10° storage. (b) Viscosity curves of PT-ABVN formulation for different days at 10° storage.

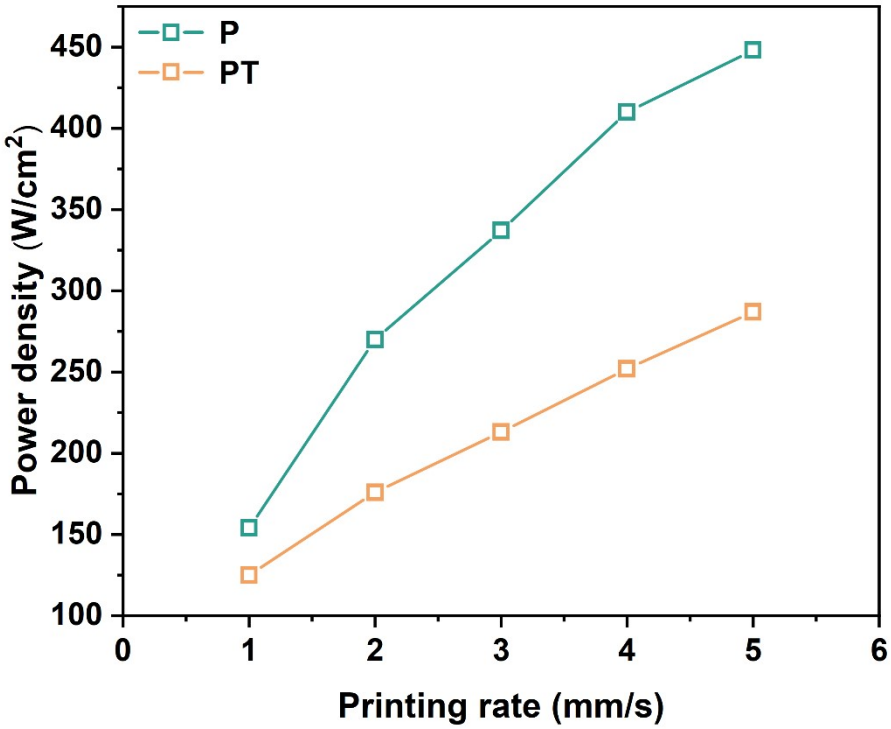

Fig. S11. Minimum laser power density for successful cantilever printing via different system inks at varying rates

Fig. S12. The columnar structure with different inclination angles printed by PTSC. The print rate is 2 mm/s, and the power density of NIR laser is 200 W/cm^2. The length of the scale bar in the figure is 1 cm.